

A multiscale Eulerian–Lagrangian localized adjoint method for transient advection–diffusion equations with oscillatory coefficients

Hong Wang · Yabin Ding · Kaixin Wang ·
Richard E. Ewing · Yalchin R. Efendiev

Received: 31 January 2005 / Accepted: 2 May 2006
© Springer-Verlag 2007

Abstract We develop a multiscale Eulerian–Lagrangian localized adjoint method for transient linear advection–diffusion equations with oscillatory coefficients, which arise in mathematical models for describing flow and transport through heterogeneous porous media, composite material design, and other applications.

Keywords Advection–diffusion equations · Eulerian–Lagrangian method · Multiscale method · Reservoir simulation · Porous medium flow

1 Introduction

Transient advection–diffusion partial differential equations arise in mathematical models for describing groundwater hydrology, environmental modeling and remediation, petroleum reservoir simulation and many other fields [2, 6, 9]. These problems admit solutions with moving steep fronts and complicated structures. Centered finite difference or finite element methods often generate numerical solutions with severe nonphysical oscillations. In industrial applications,

upstream weighting techniques are commonly used to stabilize the numerical approximations to these systems in large-scale simulators. But upwind methods tend to produce excessive numerical diffusion, which smears out moving steep fronts of the solutions to the governing equations and introduces spurious grid orientation effect [6, 17].

In addition, advection–diffusion equations for describing porous medium flow through heterogeneous porous media usually contain solutions with multiple spatial and temporal scales. Consequently, a direct numerical solution strategy often requires extremely refined space grids and time steps, due to the wide spectrum of spatial and temporal scales in the solutions and the advection–diffusion feature of the governing equations.

The Eulerian–Lagrangian localized adjoint method (ELLAM) [4] provides a general framework for developing characteristic methods to solve transient advection–diffusion equations with general boundary conditions in a mass-conservative manner. The ELLAM schemes have been successfully applied in the numerical modeling of petroleum reservoir simulation and groundwater contaminant transport and remediation. They generate accurate numerical solutions even if large time steps and spatial grids are used, and are very competitive with many numerical methods [3, 8, 14–16].

The multiscale finite element (or volume) method (MsFEM) [5, 10, 11] was introduced in recent years for solving partial differential equations with multiscale solutions. These methods aim at obtaining large scale solutions accurately and effectively without resolving small scale details. These ideas were carried out via the construction of basis functions that capture small scale information within each cell, so the effect of small scales on the large scale is captured correctly.

We develop a multiscale Eulerian–Lagrangian localized adjoint method (MsELLAM) for a transient linear

Communicated by G. Wittum.

H. Wang (✉) · Y. Ding
Department of Mathematics, University of South Carolina,
Columbia, SC 29208, USA
e-mail: hwang@math.sc.edu

K. Wang
School of Mathematics and System Sciences,
Shandong University, Jinan, Shandong 250100, China

R. E. Ewing · Y. R. Efendiev
Institute for Scientific Computation, Texas A&M University,
College Station, TX 77843-3404, USA

advection–diffusion equation with oscillatory coefficients. The goal of this paper is to expose the fundamental idea in the development of such a scheme within the framework of the ELLAM formulation and the MsFEM, so we focus on a simple model problem in most of the paper. At the end of this paper we briefly discuss extensions of the MsELLAM scheme for coupled systems modeling porous medium flow.

2 An ELLAM formulation

In this section we revisit the idea of the ELLAM framework [4] in the context of one-dimensional advection–diffusion equations with oscillatory coefficients

$$c_t + \left(V \left(x, \frac{x}{\varepsilon} \right) c - D \left(x, \frac{x}{\varepsilon} \right) c_x \right)_x = f, \tag{1}$$

$$x \in (a, b), \quad t \in (0, T],$$

where V is velocity field, D is the diffusion coefficient, f is a given source or sink term, and $c(x, t)$ is a measure of concentration of a dissolved substance. Due to the heterogeneity of the porous medium, the velocity V and diffusion coefficient D may be random or highly oscillatory. Consequently, the solution could contain multiple scales. In the model problem (1), we assume the problem to have two scales: a scale of $O(1)$ that represents the normal scale, and a scale of $O(\varepsilon)$ that represents a fast changing scale. Note that we do not impose a periodicity assumption on the problem.

The ELLAM framework can treat advection–diffusion equations with general inflow and outflow boundary conditions in a mass-conservative manner [4, 14]. Since the goal of this paper is to explore how to utilize the idea of the multiscale finite element method [10] within the ELLAM framework to design a multiscale ELLAM scheme, we skip the treatment of boundary conditions by, e.g., assuming an initial condition with compact support or periodic boundary conditions.

Equation (1) is also subject to the initial condition

$$c(x, 0) = c_0(x), \quad x \in [a, b]. \tag{2}$$

2.1 Weak formulation

We begin by defining a space–time partition:

$$x_i := a + i \Delta x, \quad 0 \leq i \leq I, \quad \Delta x := \frac{b - a}{I} \tag{3}$$

$$t_n := n \Delta t, \quad 0 \leq n \leq N, \quad \Delta t := \frac{T}{N}.$$

Due to various mathematical, numerical, and computational constraints, the size of spatial grids and time steps Δx and Δt often has to be chosen much larger than the fine scale ε in practical simulations.

We multiply Eq. (1) by space–time test functions w that vanish outside $[a, b] \times (t_{n-1}, t_n]$ and are discontinuous in

time at time step t_{n-1} and integrate the resulting equation to get

$$\int_{t_{n-1}}^{t_n} \int_a^b \left(c_t + \left(V \left(x, \frac{x}{\varepsilon} \right) c - D \left(x, \frac{x}{\varepsilon} \right) c_x \right)_x \right) w dx dt \tag{4}$$

$$= \int_{t_{n-1}}^{t_n} \int_a^b f w dx dt.$$

Integration by parts in both space and time yields a weak formulation

$$\int_a^b c(x, t_n) w(x, t_n) dx + \int_{t_{n-1}}^{t_n} \int_a^b D \left(x, \frac{x}{\varepsilon} \right) c_x w_x dx dt$$

$$- \int_{t_{n-1}}^{t_n} \int_a^b c \left(w_t + V \left(x, \frac{x}{\varepsilon} \right) w_x \right) dx dt$$

$$= \int_a^b c(x, t_{n-1}) w(x, t_{n-1}^+) dx + \int_{t_{n-1}}^{t_n} \int_a^b f w dx dt. \tag{5}$$

Here $w(x, t_{n-1}^+) := \lim_{t \rightarrow t_{n-1}^+} w(x, t)$ accounts for the discontinuity of $w(x, t)$ at time t_{n-1} .

Based on the idea of the localized adjoint method or optimal test function method [4, 12], the test functions w should be chosen from the solution space of the homogeneous adjoint equation of Eq. (1)

$$- w_t - V \left(x, \frac{x}{\varepsilon} \right) w_x - \left(D \left(x, \frac{x}{\varepsilon} \right) w_x \right)_x = 0. \tag{6}$$

2.2 Operator splitting

Because the solution space of ordinary differential equations is finite-dimensional, the development of optimal test function methods for the boundary-value problem of one-dimensional ordinary differential equations is relatively simple [4, 12]. In contrast, the solution space of the partial differential equation (6) is infinite-dimensional. Since the objective of a numerical procedure is to derive a finite-dimensional approximation, only a finite number of test functions should be chosen. Different choices of test functions lead to different classes of approximations.

2.2.1 An optimal test function operator-splitting

In the context of the adjoint equation (6), one option is to split the adjoint operator into a spatial operator and a temporal operator. Namely, we require the test functions $w(x, t)$ to satisfy the following system that consists of two sub-equations within each element $(x_{i-1}, x_i) \times (t_{n-1}, t_n]$

$(i = 1, 2, \dots, I)$

$$\begin{aligned}
 w_t &= 0, \\
 -V\left(x, \frac{x}{\varepsilon}\right)w_x - \left(D\left(x, \frac{x}{\varepsilon}\right)w_x\right)_x &= 0.
 \end{aligned}
 \tag{7}$$

The second equation in (7) is a singularly-perturbed, two-scale, steady-state advection–diffusion equation. It defines the spatial configuration of the test functions w . This type of splitting leads to a class of optimal test function methods involving exponential upstream weighting in space. The corresponding test functions w typically exhibit exponential boundary layers near the inter-element boundary, which require a fine grid for reasonable resolution. The first equation in (7) defines the temporal variation of the test functions w . Numerical methods resulting from these test functions tend to have large temporal truncation errors, numerical dispersion, and phase errors [4, 14, 15]. The combination of multiscale feature and advection dominance of the problems introduces extra numerical difficulties.

2.2.2 An Eulerian–Lagrangian operator-splitting

An alternative operator splitting of the adjoint equation (6) is to split the adjoint operator into a first-order hyperbolic operator and a second-order diffusion operator. Namely, we require the test functions $w(x, t)$ to satisfy the following system that consists of two sub-equations within each Eulerian–Lagrangian element Ω_i , which is a space–time strip emanating backward from (x_{i-1}, x_i) along the characteristics from time step t_n to time step t_{n-1}

$$\begin{aligned}
 -w_t - V\left(x, \frac{x}{\varepsilon}\right)w_x &= 0, \\
 -\left(D\left(x, \frac{x}{\varepsilon}\right)w_x\right)_x &= 0.
 \end{aligned}
 \tag{8}$$

In the ELLAM framework, the equations in (8) are imposed locally within the interior of each element Ω_i . As in the case of optimal test function splitting, the second equation in (8) defines the spatial configuration of the test functions w . This equation is now an elliptic steady-state diffusion equation, in contrast to a steady-state advection–diffusion equation. Consequently, the test functions w are not expected to exhibit boundary layers near the inter-element boundary. The first equation in (8) defines the temporal variation of the test functions w , which implies the Lagrangian feature of the test functions. We note that in the case of scale separation (e.g., problems with periodic coefficients) the solution of the local problems (7) and (8) can be approximated using auxiliary problems, which arise in homogenization. This approximation will reduce the computational cost of the proposed method.

3 An MsELLAM tracking fine-scale velocity

The objective of this section is to derive an MsELLAM for problem (1), (2) by incorporating multiscale-handling capability into the ELLAM framework.

3.1 Definition of test functions

One of the key issues in the development of MsELLAM is the choice of test functions in the ELLAM framework. In order for the MsELLAM to handle multiscale advection–diffusion equations, we utilize the idea of multiscale finite element method (MsFEM) [10] in the construction of the test functions in the MsELLAM.

3.1.1 Spatial configuration of the test functions

The second equation in the Eulerian–Lagrangian operator-splitting (8), which defines spatial configuration of the test functions w in the ELLAM framework, is a self-adjoint elliptic equation. The original MsFEM was developed for such an equation [10]. We naturally follow the idea of MsFEM to define the spatial configuration of the test functions w at time step t_n .

Because the mesh size of the coarse grid $\Delta x > \varepsilon$, the test functions in a conventional finite element method, which is linear on $[x_{i-1}, x_i]$, cannot handle fine-scale behavior of the solutions. In the MsFEM a subdivision

$$x_{i,j} := x_{i-1} + j\Delta x_f, \quad 0 \leq j \leq J, \quad \Delta x_f := \frac{\Delta x}{J} \tag{9}$$

is introduced in $[x_{i-1}, x_i]$, where $\Delta x_f = O(\varepsilon)$ is chosen to account for the fine-scale behavior. Then two piecewise-linear basis functions $w_i^{(1)}(x, t_n)$ and $w_i^{(2)}(x, t_n)$ are determined by using a finite element method to solve the second equation in (8) in $[x_{i-1}, x_i]$ with respect to the subdivision (9) and the boundary condition

$$\begin{aligned}
 w_i^{(1)}(x_{i-1}, t_n) &= 1, & w_i^{(1)}(x_i, t_n) &= 0, \\
 w_i^{(2)}(x_{i-1}, t_n) &= 0, & w_i^{(2)}(x_i, t_n) &= 1.
 \end{aligned}
 \tag{10}$$

The shape functions $w_i^{(1)}(x, t_n)$ and $w_i^{(2)}(x, t_n)$ are restricted to the element $[x_{i-1}, x_i]$, and are extended outside of the element by 0. These shape functions for $i = 0, 1, \dots, I$ form a basis for the MsFEM with the degrees of freedom being still located at coarse spatial grid nodes x_i for $i = 0, 1, \dots, I$. In this way, the basis functions naturally build the multiscale behavior into their construction and reflect the multiscale behavior due to diffusion.

3.1.2 Temporal variation of the test functions

Once the spatial configuration of the test functions $w(x, t_n)$ is determined at time step t_n , the first equation in the Eulerian–

Lagrangian splitting (8) defines the temporal variation of $w(x, t)$ from time step t_n to time step t_{n-1} by extending them backward along the characteristic curves $y = r(t; x, t_n)$ defined by

$$\begin{aligned} \frac{dy}{dt} &= V\left(y, \frac{y}{\varepsilon}\right), \\ y\Big|_{t=t_n} &= x. \end{aligned} \tag{11}$$

In the case of multiscale transient advection–diffusion equations, the velocity field exhibits multiscale or oscillatory behavior. Consequently, the evaluation of the test functions w , which is carried out via a characteristic tracking, requires an accurate resolution of problem (11) determined by the fine-scale velocity field V . Since the size of the global time step $\Delta t > \varepsilon$, we introduce a local time-step partition

$$t_{n,k} := t_{n-1} + k\Delta t_f, \quad 0 \leq k \leq K, \quad \Delta t_f := \frac{\Delta t}{K} \tag{12}$$

where the size of the local time step $\Delta t_f = O(\varepsilon)$ is chosen to handle the multiscale behavior in time.

3.2 Numerical scheme

With the test functions defined in Sect. 3.1, we now derive an MsELLAM scheme. For clarity of exposition, we use the variable y to represent the spatial coordinate of any point in the domain. We use the change of variable $y = r(\theta; x, t_n)$ to evaluate the source term in Eq. (5) to obtain

$$\begin{aligned} &\int_{\Omega_i} \int f(y, t)w(y, t)dydt \\ &= \int_{t_{n-1}}^{t_n} \int_{r(t; x_{i-1}, t_n)}^{r(t; x_i, t_n)} f(y, t)w(y, t)dydt \\ &= \sum_{k=1}^K \int_{t_{n,k-1}}^{t_{n,k}} \int_{r(t; x_{i-1}, t_n)}^{r(t; x_i, t_n)} f(y, t)w(y, t)dydt. \end{aligned} \tag{13}$$

Then we can use a numerical quadrature to discretize the temporal integral on each local time interval $[t_{n,k-1}, t_{n,k}]$ for $k = 1, 2, \dots, K$.

We handle the diffusion term in a similar manner

$$\begin{aligned} &\int_{\Omega_i} \int D\left(y, \frac{y}{\varepsilon}\right)c_y(y, t)w_y(y, t)dydt \\ &= \int_{t_{n-1}}^{t_n} \int_{r(t; x_{i-1}, t_n)}^{r(t; x_i, t_n)} D\left(y, \frac{y}{\varepsilon}\right)c_y(y, t)w_y(y, t)dydt \\ &= \sum_{k=1}^K \int_{t_{n,k-1}}^{t_{n,k}} \int_{r(t; x_{i-1}, t_n)}^{r(t; x_i, t_n)} D\left(y, \frac{y}{\varepsilon}\right)c_y(y, t)w_y(y, t)dydt. \end{aligned} \tag{14}$$

Because the test functions w satisfy the first equation of (8) (at least approximately), the last term on the left-hand side of (5) vanishes (or at least is the same order as the global truncation error of the numerical scheme [7, 13]). Hence, we drop this term in the numerical scheme. We then obtain an MsELLAM scheme by incorporating Eqs. (13) and (14) into Eq. (5).

4 An MsELLAM tracking coarse-scale velocity

The MsELLAM scheme developed in the previous section requires a characteristic tracking of the fine-scale velocity field. In this section we explore the possibility of developing an MsELLAM for problem (1), (2), which requires only tracking the coarse-grid velocity field.

4.1 Definition of test functions

One of the key issues in the development of MsELLAM is the choice of test functions in the ELLAM framework, which in turn is the result of an appropriate operator-splitting.

4.1.1 An alternative Eulerian–Lagrangian operator-splitting

To develop an MsELLAM scheme that requires only tracking the coarse-grid velocity field, we decompose the fine-scale velocity field V as

$$V = \bar{V} + \tilde{V}. \tag{15}$$

Here \bar{V} and \tilde{V} represent the global, smooth part and the local, oscillatory part of the velocity field V , respectively.

We revise the Eulerian–Lagrangian operator-splitting (8) as follows

$$\begin{aligned} -w_t - \bar{V}w_x &= 0, \\ -\tilde{V}_x - (Dw_x)_x &= 0. \end{aligned} \tag{16}$$

In the ELLAM framework, the equations in (8) are imposed locally within the interior of each element Ω_i . We note that a somewhat related modified Eulerian–Lagrangian operator-splitting was previously used in [7] for the purpose of improving the accuracy of the numerical approximation and simplifying the characteristic tracking algorithm.

4.1.2 Spatial configuration of the test functions

We note that the second equation in the operator-splitting (16) is now a steady-state advection–diffusion equation. We use the MsFEM idea to define the spatial configuration of the basis functions w at time step t_n . In the current context, we solve the second equation in (16) by a standard finite element method with the fine-scale subdivision (9) on interval

$[x_{i-1}, x_i]$. Because the fine-scale grid size $\Delta x_f = O(\varepsilon)$ is chosen to be small enough so that the grid Peclet number is of $O(1)$, we do not expect that the basis functions exhibit nonphysical oscillations [12].

4.1.3 Temporal variation of the test functions

Once the spatial configuration of the test functions $w(x, t_n)$ is determined at time step t_n , the first equation in the modified Eulerian–Lagrangian splitting (16) defines the temporal variation of $w(x, t)$ from time step t_n to time step t_{n-1} by extending them backward along the characteristic curves $y = r(t; x, t_n)$ defined by

$$\begin{aligned} \frac{dy}{dt} &= \tilde{V}\left(y, \frac{y}{\varepsilon}\right), \\ y\Big|_{t=t_n} &= x. \end{aligned} \tag{17}$$

4.2 Numerical scheme

The diffusion term and source term in the reference equation (5) can be handled in a similar manner to Eqs. (13) and (14). The first equation in the modified Eulerian–Lagrangian operator-splitting (16) implies

$$\int_{t_{n-1}}^{t_n} \int_a^b c(w_t + \tilde{V}w_x) dx dt \tag{18}$$

vanishes, or at least, is within the global truncation error of the numerical scheme [7]. The oscillatory part \tilde{V} of the velocity field on the left-hand side of the reference equation (5) remains, which can be approximated as follows

$$\begin{aligned} &\int_{\Omega_i} \int \tilde{V}\left(y, \frac{y}{\varepsilon}\right) c(y, t) w_y(y, t) dy dt \\ &= \int_{t_{n-1}}^{t_n} \int_{r(t; x_{i-1}, t_n)}^{r(t; x_i, t_n)} \tilde{V}\left(y, \frac{y}{\varepsilon}\right) c(y, t) w_y(y, t) dy dt \\ &= \sum_{k=1}^K \int_{t_{n,k-1}}^{t_{n,k}} \int_{r(t; x_{i-1}, t_n)}^{r(t; x_i, t_n)} \tilde{V}\left(y, \frac{y}{\varepsilon}\right) c(y, t) w_y(y, t) dy dt. \end{aligned} \tag{19}$$

We handle the temporal integral in this term as we did with the source term in Eq. (13) and with the diffusion term in (14) in Sect. 3.

5 Numerical experiments

We simulate the transport of a one-dimensional Gaussian pulse over the spatial domain $[0, 4]$. In the example runs the time interval is $[0, T] = [0, 1]$. The initial condition is given

by

$$c_0(x) = \exp\left(-\frac{(x - x_0)^2}{2\sigma^2}\right), \tag{20}$$

where the center $x_0 = 0.5$ and the spread $\sigma = 0.1$ that determines the steepness of the Gaussian pulse.

A two-scale oscillatory velocity field $V(x/\varepsilon)$ and diffusion coefficient $D(x/\varepsilon)$ is chosen as follows

$$\begin{aligned} V\left(\frac{x}{\varepsilon}\right) &= 1 + \alpha \cos\left(\frac{2\pi x}{\varepsilon}\right), \\ D\left(\frac{x}{\varepsilon}\right) &= \frac{0.01}{1 + 0.8 \sin\left(\frac{2\pi x}{\varepsilon}\right)}, \end{aligned} \tag{21}$$

where $\alpha = 0.2$ which determines the magnitude of the oscillatory velocity field. We use $\varepsilon = 0.02, 0.01$ and 0.005 to investigate the convergence rate. The source term f is chosen to be zero.

5.1 Results with ELLAM

We use an ELLAM scheme with extremely refined spatial grid and time step to generate a reference solution, which is presented in Fig. 1. In Table 1 and Fig. 1 we present numerical results generated by an ELLAM scheme with an accurate characteristics tracking using a second-order Runge–Kutta formula. These numerical results show that the ELLAM scheme converges only when the meshsize $\Delta x < \varepsilon$. This is fully understandable and can be explained as follows. Although ELLAM schemes have been successfully applied to simulate transient advection–diffusion equations in different applications [3,8,14–16], they are not designed to solve advection–diffusion equations with multiple scales. This is similar to the case why conventional finite element methods do not work well for multiscale elliptic equations.

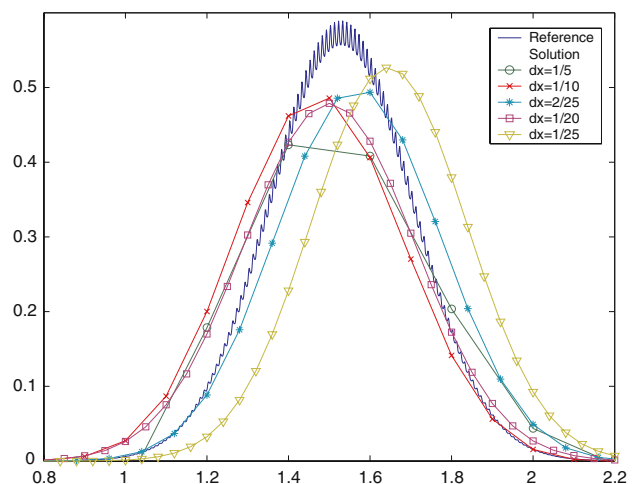


Fig. 1 Results by an ELLAM scheme with different grids

Table 1 Results with an ELLAM ($\varepsilon = \frac{1}{100}$, $\Delta t = \frac{1}{1000}$)

Δx	L_1 error	L_2 error	L_∞ error
$\frac{1}{5}$	0.0809	0.0784	0.1758
$\frac{4}{25}$	0.0888	0.0908	0.1981
$\frac{1}{10}$	0.0651	0.0753	0.1432
$\frac{2}{25}$	0.0518	0.0602	0.1202
$\frac{1}{20}$	0.0499	0.0564	0.1225
$\frac{1}{25}$	0.1269	0.1390	0.2263
$\frac{1}{50}$	0.0346	0.0390	0.0729
$\frac{1}{100}$	0.0581	0.0644	0.1376
$\frac{2}{250}$	0.0484	0.0551	0.1229
$\frac{1}{200}$	0.0260	0.0297	0.0609
$\frac{1}{250}$	0.0153	0.0182	0.0484
$\frac{1}{500}$	0.0045	0.0054	0.0150

This is the reason why we use the idea of MsFEM to develop an MsELLAM scheme.

5.2 Results of the MsELLAM tracking fine-scale velocity

In Table 2 we present the numerical results obtained by the MsELLAM scheme that requires tracking characteristic curves defined by the fine-scale velocity. In these numerical example runs the size Δx of the coarse spatial grid varies from $\frac{1}{5}$ to $\frac{1}{100}$. The size of the fine spatial grid Δx_f is chosen to be fixed $\Delta x_f = \frac{1}{1000}$. We choose the size Δt of the coarse temporal step is chosen to be $\Delta t = \Delta x$. The size Δt_f of the fine-scale temporal step is chosen to be $\Delta t_f = \Delta x_f$.

The numerical results in Table 2 and Fig. 2 show that the MsELLAM converges for $\Delta x > \varepsilon$. As Δx is close to ε , the MsELLAM does not converge due to resonance effect [10]. In other words, the MsELLAM exhibits the same convergence behavior for multiscale transient advection–diffusion equations as the MsFEM for multiscale elliptic equations.

Table 2 Results with the MsELLAM scheme tracking fine-scale velocity ($\varepsilon = \frac{1}{100}$)

Δx	L_1 error	L_2 error	L_∞ error
$\frac{1}{5}$	0.0803	0.0743	0.1590
$\frac{1}{10}$	0.0163	0.0208	0.0624
$\frac{1}{20}$	0.0103	0.0130	0.0365
$\frac{1}{25}$	0.0101	0.0125	0.0345
$\frac{1}{50}$	0.0099	0.0122	0.0319
$\frac{1}{100}$	0.0099	0.0121	0.0315

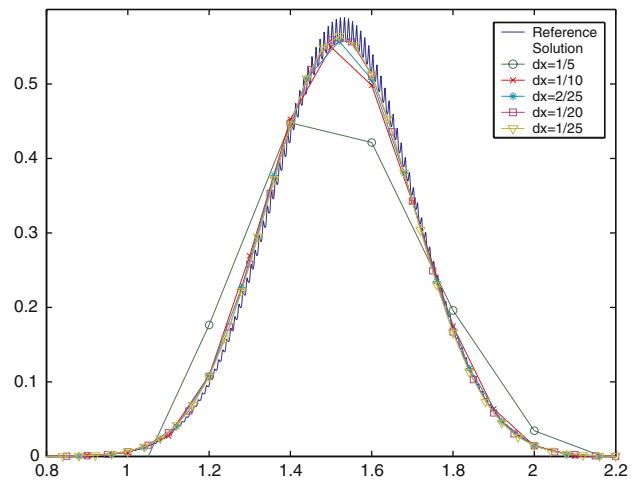


Fig. 2 Results of MsELLAM tracking fine-scale velocity

5.3 Results of the MsELLAM tracking coarse-scale velocity

We present the numerical results generated by the MsELLAM scheme that just track the coarse-scale velocity in Table 3 and Fig. 3. We see that this scheme generates simi-

Table 3 Results of the MsELLAM tracking coarse-scale velocity ($\varepsilon = \frac{1}{100}$)

Δx	L_1 error	L_2 error	L_∞
$\frac{1}{5}$	0.0801	0.0739	0.1584
$\frac{1}{10}$	0.0158	0.0202	0.0616
$\frac{1}{20}$	0.0095	0.0123	0.0358
$\frac{1}{25}$	0.0093	0.0118	0.0330
$\frac{1}{50}$	0.0092	0.0114	0.0305
$\frac{1}{100}$	0.0092	0.0114	0.0301

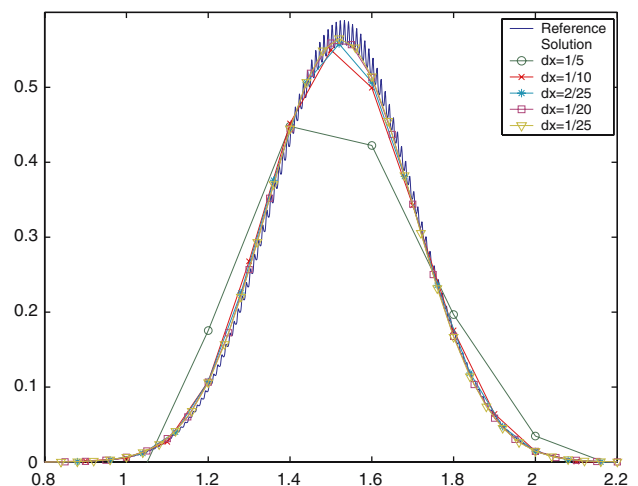


Fig. 3 MsELLAM velocity splitting scheme with different meshsize

lar results as the MsELLAM scheme requiring tracking the fine-scale velocity, even though only the coarse-scale velocity is tracked.

6 Discussion and future work

We developed a multiscale Eulerian–Lagrangian localized adjoint method (MsELLAM) for time-dependent advection–diffusion equations with highly oscillatory coefficients. Preliminary numerical experiments have shown the potential of these MsELLAM schemes. Although we restrict the development of the MsELLAM to a simple one-dimensional advection–diffusion equation, our goal is to develop an MsELLAM for coupled systems in porous medium flow. We take the system of single-phase flow as an example to demonstrate the idea.

Let $c(\mathbf{x}, t)$ be the concentration of an invading fluid and let $p(\mathbf{x}, t)$ and $\mathbf{u}(\mathbf{x}, t)$ be the pressure and Darcy velocity of the fluid mixture. The mass conservation equation for the fluid mixture incorporated with the incompressibility condition, Darcy’s law, and the mass conservation equation for the invading fluid lead to the following coupled system of PDEs [2, 6]

$$\begin{aligned} \nabla \cdot \mathbf{u} &= q, & \mathbf{u} &= -\frac{\mathbf{K}}{\mu(c)} \nabla p, \\ \phi c_t + \nabla \cdot (\mathbf{u}c - \mathbf{D}(\mathbf{x}, \mathbf{u})\nabla c) &= \bar{c}q, & \mathbf{x} \in \Omega, \quad t \in [0, T]. \end{aligned} \tag{22}$$

System (22) models miscible displacement of one incompressible fluid by another or groundwater contaminant transport through a two-dimensional horizontal porous medium reservoir Ω over a time period of $[0, T]$. In this system $\mathbf{K}(\mathbf{x})$ is the 2×2 permeability tensor of the medium, $\mu = \mu(c)$ is the concentration-dependent viscosity of the fluid mixture, $q(\mathbf{x}, t)$ is the external source and sink term, $\phi(\mathbf{x})$ is the porosity of the medium, $\mathbf{D}(\mathbf{x}, \mathbf{u})$ is the diffusion-dispersion tensor. $\bar{c}(\mathbf{x}, t)$ is either the specified concentration of the injected fluid at sources or $\bar{c}(\mathbf{x}, t) = c(\mathbf{x}, t)$ is the resident concentration at sinks.

The first two equations in system (22) form a second-order elliptic equation for the pressure p . For heterogeneous porous media, $\mathbf{K}(\mathbf{x})$ exhibit multiscale behavior. The multiscale finite element or volume method developed in [10, 11] can be applied to solve the pressure equation. In fact, the MsFEM framework can be improved to take the full advantage of the physical and mathematical properties of the porous medium flow. The basic idea can be summarized as follows [1]:

At time $t = 0$, the MsFEM basis functions are constructed by using a finite element method to solve the homogeneous

pressure equation

$$-\nabla \cdot (\mathbf{K}\nabla p) = 0 \tag{23}$$

on each spatial cell with a fine-scale subdivision. The construction of the MsFEM basis functions is usually an expensive process. Note that the viscosity $\mu = \mu(c)$ changes very little in majority of the physical domain Ω , where the concentration c is smooth. μ changes rapidly within the neighborhood of the moving steep front region. Hence, in most of the domain Ω where c is smooth

$$-\nabla \cdot \left(\frac{\mathbf{K}}{\mu(c)} \nabla p \right) \approx -\frac{1}{\mu(c)} \nabla \cdot (\mathbf{K}\nabla p). \tag{24}$$

In other words, the MsFEM basis functions constructed at time $t = 0$ can still be used at later time steps. One needs only to update the MsFEM basis functions in the region with moving steep fronts.

We notice that similar arguments work for the transport equation in the system (22). So the spatial configurations of the MsELLAM basis functions constructed at time $t = 0$ can be used at later time steps, except within the region with moving steep fronts where the MsELLAM basis functions need to be updated. The temporal variation of the test functions is evaluated via a characteristic tracking, which is needed in the evaluation of other terms in the MsELLAM schemes anyway. Moreover, the characteristic tracking is local and is fully parallelizable. We will pursue our research in this direction in the near future.

Finally, we address some implementational issues in the context of the MsELLAM for multiscale advection–diffusion equations in multiple space dimensions. In the MsELLAM, the spatial integrals on each coarse cell are evaluated via a numerical quadrature on every fine cell in the coarse cell. A forward tracking algorithm seems to be a feasible choice in this case. The option of tracking a coarse velocity field seems more attractive, since it greatly simplifies the tracking procedure and avoids the inter-element boundary layer of the basis functions. Numerically, the coarse velocity field is often chosen as the mean velocity field on the coarse mesh. As pointed out in [10], an oversampling technique could be used to compute the shape functions on a slightly larger domain to avoid boundary layers in multiple space dimensions.

Acknowledgements This research is partially supported by NSF CMG/DMS grant 0621113, DOE grant DE-FG02-06ER25727, National Natural Science Foundation of China No. 10771124, and the Research Fund for Doctoral Program of High Education by Station Education Ministry of China No. 20060422006.

References

1. Aarnes, J., Espedal, M.S.: A new approach to upscaling for two-phase flow in heterogeneous porous media. Fluid flow and transport in porous media: mathematical and numerical treatment, 1–11,

- Contemp. Math., 295, American Mathematical Society, Providence, RI (2002)
2. Bear, J.: Dynamics of Fluids in Porous Materials. Elsevier, New York (1972)
 3. Binning, P.J., Celia M.A.: A finite volume Eulerian–Lagrangian localized adjoint method for solution of the contaminant transport equations in two-dimensional multi-phase flow systems. *Water Resour. Res.* **32**, 103–114 (1996)
 4. Celia, M.A., Russell, T.F., Herrera, I., Ewing, R.E.: An Eulerian–Lagrangian localized adjoint method for the advection–diffusion equation. *Adv. Water Resour.* **13**, 187–206 (1990)
 5. Efendiev, Y.R., Hou, T.Y., Wu, X.H.: Convergence of a non-conforming multiscale finite element method. *SIAM J. Numer. Anal.* **37**, 888–910 (2000)
 6. Ewing, R.E. (eds.): The Mathematics of Reservoir Simulation. Research Frontiers in Applied Mathematics, 1, SIAM, Philadelphia (1984)
 7. Ewing, R.E., Wang, H.: An optimal-order error estimate to Eulerian–Lagrangian localized adjoint method for variable-coefficient advection reaction problems. *SIAM Numer. Anal.* **33**, 318–348 (1996)
 8. Healy, R.W., Russell, T.F.: Solution of the advection-dispersion equation in two dimensions by a finite-volume Eulerian–Lagrangian localized adjoint method. *Adv. Water Res.* **21**, 11–26 (1998)
 9. Helmig, R.: Multiphase Flow and Transport Processes in the Sub-surface. Springer, Berlin (1997)
 10. Hou, T.Y., Wu, X.H.: A multiscale finite element method for elliptic problems in composite materials and porous media. *J. Comput. Phys.* **134**, 169–189 (1997)
 11. Jenny, P., Lee, S.H., Tchelepi, H.A.: Multiscale finite-volume method for elliptic problems in subsurface flow simulation. *J. Comput. Phys.* **187**, 47–67 (2003)
 12. Roos, H.-G., Stynes, M., Tobiska, L.: Numerical Methods for Singularly Perturbed Differential Equations. Springer, Berlin (1996)
 13. Wang, H.: A family of ELLAM schemes for advection–diffusion reaction equations and their convergence analyses. *Numer. Methods for PDEs* **14**, 739–780 (1998)
 14. Wang, H., Dahle, H.K., Ewing, R.E., Espedal, M.S., Sharpley, R.C., Man, S.: An ELLAM Scheme for advection–diffusion equations in two-dimensions. *SIAM J. Sci. Comput.* **20**, 2160–2194 (1999)
 15. Wang, H., Ewing, R.E., Qin, G., Lyons, S.L., Al-Lawatia, M., Man, S.: A family of Eulerian–Lagrangian localized adjoint methods for multi-dimensional advection reaction equations. *J. Comput. Phys.* **152**, 120–163 (1999)
 16. Wang, H., Liang, D., Ewing, R.E., Lyons, S.L., Gin, G.: An approximation to miscible fluid flows in porous media with point sources and sinks by an Eulerian–Lagrangian localized adjoint method and mixed finite element methods. *SIAM J. Sci. Comput.* **22**, 561–581 (2000)
 17. Yanosik, J., McCracken, T.: A nine-point, finite difference reservoir simulator for realistic prediction of adverse mobility ratio displacements. *Soc. Pet. Eng. J.* **19**, 253–262 (1978)